ORIGINAL ARTICLE

ORAL DISEASES · WILEY

Functional study of novel *PAX9* variants: The paired domain and non-syndromic oligodontia

Kai Sun[1] | Miao Yu[1] | Iting Yeh[1] | Liutao Zhang[1] | Haochen Liu[1] | Tao Cai[2,3] | Hailan Feng[1] | Yang Liu[1] | Dong Han[1]

[1]Department of Prosthodontics, Peking University School and Hospital of Stomatology and National Clinical Research Centre for Oral Diseases and National Engineering Laboratory for Digital and Material Technology of Stomatology and Beijing Key Laboratory of Digital Stomatology, Beijing, China

[2]Experimental Medicine Section, National Institute of Dental and Craniofacial Research, National Institutes of Health, Bethesda, Maryland, USA

[3]Laboratory of Biochemistry and Genetics, NIDDK/NIH, Bethesda, Maryland, USA

Correspondence
Dong Han and Yang Liu, Department of Prosthodontics, Peking University School and Hospital of Stomatology, Beijing, China.
Emails: donghan@bjmu.edu.cn (D.H.); pkussliuyang@bjmu.edu.cn (Y.L.)

Funding information
National Natural Science Foundation of China, Grant/Award Number: 81600846, 81771054 and 81970902

Abstract

Objectives: To investigate pathogenic variants of the *paired box 9* (*PAX9*) gene in patients with non-syndromic oligodontia, and the functional impact of these variants.

Subjects and Methods: Whole exome sequencing and Sanger sequencing were utilized to detect gene variants in a cohort of 80 patients diagnosed with non-syndromic oligodontia. Bioinformatic and conformational analyses, fluorescence microscopy and luciferase reporter assay were employed to explore the functional impact.

Results: We identified three novel variants in the *PAX9*, including two frameshift variants (c.211_212insA; p.I71Nfs*246 and c.236_237insAC; p.T80Lfs*6*), and one missense variant (c.229C > G; p.R77G). Familial co-segregation verified an autosomal-dominant inheritance pattern. Conformational analyses revealed that the variants resided in the paired domain, and could cause corresponding structural impairment of the PAX9 protein. Fluorescence microscopy showed abnormal subcellular localizations of frameshift variants, and luciferase assay showed impaired downstream transactivation activities of the *bone morphogenetic protein 4* (*BMP4*) gene in all variants.

Conclusions: Our findings broaden the spectrum of *PAX9* variants in patients with non-syndromic oligodontia and support that paired domain structural impairment and the dominant-negative effect are likely the underlying mechanisms of *PAX9*-related non-syndromic oligodontia. Our findings will facilitate genetic diagnosis and counselling, and help lay the foundation for precise oral health therapies.

KEYWORDS
functional analysis, non-syndromic oligodontia, *PAX9* variants, tooth agenesis

1 | INTRODUCTION

Tooth agenesis (TA) is the developmental failure of permanent dentition and is reported to be one of the most prevalent development-related anomalies with a prevalence of 2.2%–10.1% in humans (Polder et al., 2004; Zhang et al., 2015). Oligodontia is a severer TA condition of more than six missing teeth when the third molars are excluded. This condition clinically manifests either as non-syndromic oligodontia (NSO) or as part of a syndrome (syndromic oligodontia; SO). Compared with hypodontia (one to five missing teeth), patients with oligodontia present more serious dentition defects and have worse health-related quality of life due to decreased masticatory function, phonetic ability and maxillofacial aesthetics (Vieira et al., 2004).

Genetic, environmental and epigenetic factors are common causes of TA; however, genetics is considered to be the most

significant factor (Liu et al., 2013; Wang et al., 2016). A cluster of genes responsible for tooth morphogenesis can lead to non-syndromic tooth agenesis (NSTA), including *wingless-type MMTV integration site family member 10B* (*WNT10B*; OMIM *601906), *MSH homeobox 1* (*MSX1*; OMIM *142983), *paired box gene 9* (*PAX9*; OMIM *167416), *wingless-type MMTV integration site family member 10A* (*WNT10A*; OMIM *606268), *ectodysplasin A* (*EDA*; OMIM *300451) and *axis inhibitor 2* (*AXIN2*; OMIM *604025) (Bergendal et al., 2011; Wong, et al., 2014; Yu et al., 2016; Zeng et al., 2017). Among them, *PAX9* is one of the earliest confirmed genes associated with NSTA in an autosomal-dominant manner (TOOTH AGENESIS, SELECTIVE, 3; STHAG3; OMIM #604625) (Stockton et al., 2000). After Stockton et al. first identified a *PAX9* variant in patients with a distinct manifestation of molar oligodontia, more attentions were paid to the *PAX9* variants and oligodontia, and henceforth, a series of tooth agenesis phenotypes in NSO patients with defined *PAX9* variants were reported. (Jumlongras et al., 2004; Lammi et al., 2003; Nieminen et al., 2001; Thimmegowda et al., 2015; Wong et al., 2018).

As a well-known transcription factor, *PAX9* serves as a principle regulator during embryonic developmental processes, especially tooth development (Peters et al., 1998). The gene contains 4 exons that encode for 341 amino acids to form the PAX9 protein, which specifically binds to downstream DNA promoter regions by the DNA-binding paired domain (PD) (Wong et al., 2018). The PD is an important functional domain and has a bipartite structure composed of two distinct helix-turn-helix motifs (a N-subdomain and a C-subdomain connected by a linker). Recognition of the target DNA by PAX9 protein (PD-DNA contact) is realized through the coordination of these two subdomains (Vogan & Gros, 1997), and thereby activates odontogenic potential during tooth morphogenesis and the following tooth formation process (Jia et al., 2013). Evidence from murine studies has confirmed that homozygous *Pax9*-deficient mice present a failure in tooth development due to its arrest at the bud stage, suggesting an indispensable role of *Pax9* in tooth mesenchymal establishment and bud-to-cap patterning (Peters et al., 1998).

Although approximately 50 pathogenic variants have so far been identified in *PAX9* that lead to NSO (Bonczek et al., 2017; Daw et al., 2017; Koskinen et al., 2019; Sarkar et al., 2017; Wong et al., 2018; Zhang et al., 2019), novel variants continue to be identified, and the definite pathogenic mechanism underlying *PAX9*-related NSO has not yet been elucidated. In this study, we sought to provide more evidence to address this important issue. We employed whole exome sequencing (WES) and Sanger sequencing to identify potential genetic defects among 80 individuals with NSO. We then used bioinformatic and conservation analyses to predict the pathogenicity of identified variants. Finally, we conducted conformational structural analysis and preliminary functional studies to further investigate the possible effects of these altered PAX9 proteins in vitro.

2 | SUBJECTS AND METHODS

2.1 | Recruitment of patients with NSO

A cohort of 80 non-consanguineous individuals with NSO was recruited from the Department of Prosthodontics at the Peking University Hospital of Stomatology. Physical examination, intra-oral and panoramic radiographic examinations were performed. No missing permanent teeth were claimed to be caused by injury or extraction. All participants provided written informed consent for the academic purposes of clinical photographs and follow-up genetic analyses. All experiments were approved by the Ethics Committee of Peking University School and Hospital of Stomatology (PKUSSIRB-201736082) and performed in accordance with the principles of the Declaration of Helsinki.

2.2 | Genetic tests and variant analysis

Genomic DNA of the patients and of their available family members were obtained from the peripheral blood using a Universal Genomic DNA Kit (Cwbiotech), according to the manufacturer's instructions. After polymerase chain reaction (PCR), DNA products were sheared to acquire 150 to 200-bp fragments. Library preparation was conducted using Fast Library Prep Kit (iGeneTech). WES was conducted using Illumina X10 sequencing platform (Illumina) by the iGeneTech Institute. Then, we filtered the detected variants according to the following methods. Firstly, all genes associated with tooth development were analysed (Prasad et al., 2016); secondly, non-synonymous single nucleotide variants (SNVs) and insertions/deletions (InDels) with a minor allele frequency (MAF) ≥ 0.01 in bioinformatic databases, including the single nucleotide polymorphism database (dbSNP, http://www.ncbi.nlm.nih.gov/projects/SNP/snp_summary.cgi), the Genome Aggregation Database (gnomAD, http://gnomad.broadinstitute.org), the Exome Aggregation Consortium (ExAC, http://exac.broadinstitute.org) and the 1,000 Genomes Project data in Ensembl (http://asia.ensembl.org/Homo_sapiens/Info/Index) were excluded; finally, pathogenicity of the remaining variants was further predicted using the Protein Variation Effect Analyzer (PROVEAN, http://provean.jcvi.org/index.php) and polymorphism phenotyping (PolyPhen-2, http://genetics.bwh.harvard.edu/pph2/). To verify the variants and to analyse the familial co-segregation, PCR was employed to amplify four coding exons and intron–exon boundaries of the *PAX9* gene (NM_001372076.1) (primers and PCR conditions were shown in Table S1). The PCR products were sent to Tsingke Biological for purification and Sanger sequencing. TA clone sequencing was employed for the confirmation of frameshift variants.

2.3 | Conservation and protein conformation analyses

Conservation analysis of the PAX9 missense variant in different species was performed using ClustalW2 (http://www.ebi.ac.uk/tools/clustalw2/). The homo crystal scaffold of PD was obtained from SWISS-MODEL (https://swissmodel.expasy.org). Then, the influence of PAX9 variants on protein conformation was visualized using the PyMOL Molecular Graphics System (DeLano Scientific).

2.4 | Preparation of expression and reporter plasmids

The human *PAX9* gene coding sequence was subcloned into pEGFP-N1 expression vector (Tsingke Biological) between 5′-HindIII and 3′-PstI sites to construct the wild-type plasmid. The QuikChange Lightning Site-Directed Mutagenesis Kit (Agilent) was used to induce R77G mutagenesis. Insertion of A and AC nucleotides was also performed by the site-directed mutagenesis system to construct I71Nfs*246 and T80Lfs*6 frameshift variant plasmids. Next, to construct the reporter plasmid (p.2.4 *BMP4*-Luc), *BMP4* promoter sequence was linked between the 5′-*Nhe*I and 3′-*Xho*I sites of the pGL3-Basic vector (Promega). All constructed plasmids were verified by re-sequencing and BLAST tool analysis.

2.5 | Cell culture, transient transfection and Western blotting

Dulbecco's modified Eagle medium (Invitrogen) supplemented with 10% foetal bovine serum (ScienCell) and 1% penicillin–streptomycin (Solarbio) was used for culturing 293T cells at 37°C in a humidified atmosphere. Transient transfections were performed using Lipofectamine™ 3000 Transfection Reagent (Invitrogen). To verify expression, 20 μg of cell lysate protein from each group was collected for Western blotting. Blots were probed with anti-GFP antibody (ab183734; Abcam) and anti-GAPDH antibody (KM9002T; Syngene Biotech). Protein bands were visualized using ECL reagent (Thermo Scientific) and imaged.

2.6 | Fluorescence microscopy

Forty-eight hours after transfection, the 293T cells were fixed with 4% paraformaldehyde, mounted using mounting medium with 4′,6′-diamidino-2-phenylindole (DAPI; ZSGB-BIO) to stain the nuclear, and observed using a Zeiss LSM710 confocal microscope (Carl Zeiss) with a × 40/1.00 numerical aperture oil objective lens.

2.7 | Luciferase reporter assay

Wild type and variants were separately co-transfected with p.2.4 *BMP4*-Luc and *Renilla* plasmids (phRL-TK; used as the internal control). Forty-eight hours after transfection, cells were lysed for the measurement of Firefly/Renilla luciferase activity by the Dual-Luciferase Reporter Assay (Promega). Measurements were repeated at least thrice. Data were analysed by Student's *t* test using GraphPad Prism6. Quantitative results were expressed as mean ± standard deviation (*SD*), with $p < .05$ being considered statistically significant.

3 | RESULTS

3.1 | Clinical findings of patients harbouring novel PAX9 variants

In this study, 80 patients with NSO from unrelated families were involved in the analyses. Since all patients were carefully examined and did not present any systemic phenotype besides the oligodontia, they were clinically diagnosed with NSO. We conducted intra-oral examinations and panoramic radiographs to confirm our diagnoses. Unfortunately, some of the probands' family members had undergone varying degrees of dental prosthetic treatment and thus could not provide detailed numbers regarding congenital absence of teeth. WES data are available at the NCBI SRA database (www.ncbi.nlm.nih.gov/sra/) with the accession number PRJNA638099.

The proband of family #480 (II-2) was a 14-year-old girl. Clinical examination and panoramic radiograph revealed that, in addition to retained deciduous teeth, she was missing a total of 18 permanent teeth including five incisors, two upper canines, three premolars and all molars (Figure 1a). This patient provided a family history of her father and elder sister that were congenitally missing permanent teeth (Figure 2a).

The proband of family #356 (II-1) was a 22-year-old female. Her clinical and radiographic examination revealed oligodontia with agenesis of 16 permanent teeth including two lower incisors, one upper canine, five premolars and all molars (Figure 1b). This proband's mother was also diagnosed with NSO, while her father was normal (Figure 2b).

The proband of family #348 (IV-2) was a 22-year-old male who had congenital agenesis of three upper anterior teeth, four premolars and six molars (Figure 1c). The proband's elder sister, father and three agnate relatives also had an NSO phenotype (Figure 2c).

3.2 | Identification of three novel variants

Through a combination of WES and Sanger sequencing, we identified three novel PAX9 (NM_001372076.1, NP_001359005.1) variants in the PD domain (Figure 3a). Sequencing results of these variants, consisting of two frameshift variants (c.211_212insA; p.I71Nfs*246 and c.236_237insAC; p.T80Lfs*6) and one missense variant (c.229C > G; p.R77G), are shown in Figure 2. None of these variants were found in the dbSNP, 1000G, gnomAD or ExAC databases, indicating that all *PAX9* variants identified in this study were novel variants (Table 1). All these *PAX9* variants were inherited from the probands' fathers or mothers, which was confirmed by Sanger sequencing and familial
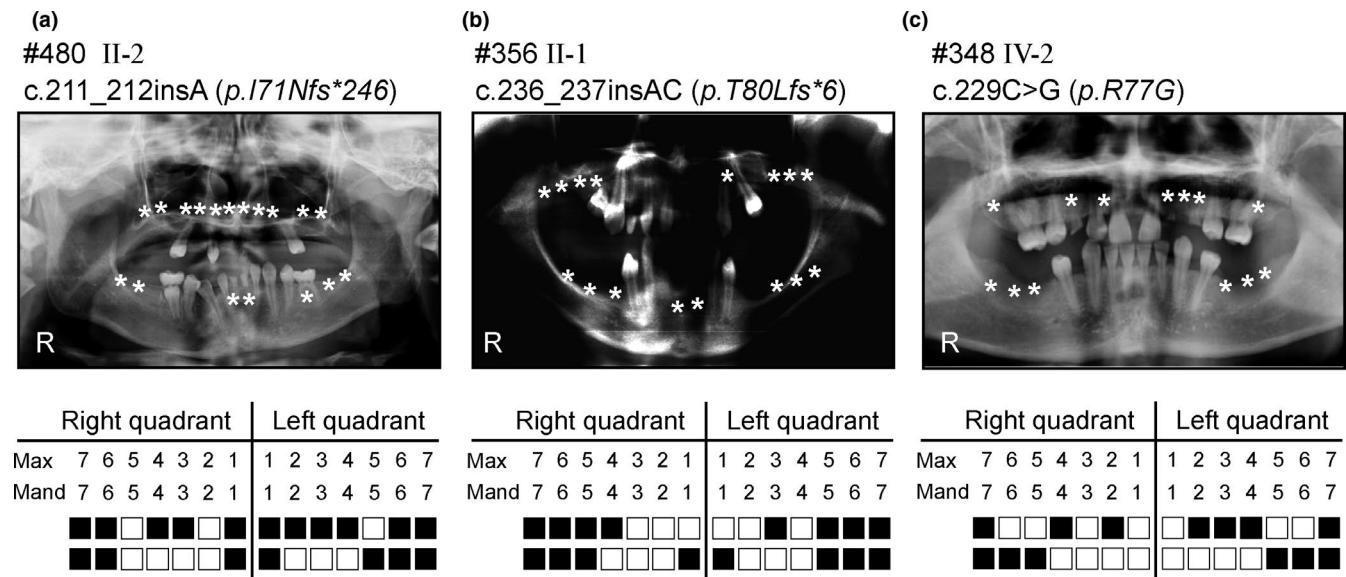
FIGURE 1 Dental features of NSO probands with *PAX9* variants. (a–c) Panoramic radiographs and schematics of oligodontia in the proband of family #480 (a), family #356 (b) and family #348 (c). White asterisks in panoramic radiographs and black solid squares in schematics indicate the congenital missing permanent teeth. R, right side; Max, maxillary; Mand, mandibular

co-segregation analysis (Figure 2 and Table 1), indicating that inheritance of *PAX9*-related NSO occurred in an autosomal-dominant manner. A summary of the above variants, locations, tooth agenesis phenotypes, possible pathogenicities and ACMG Classification (Richards et al., 2015) is presented in Table 1 and described below.

For the proband of family #480, genetic analysis demonstrated a heterozygous frameshift variant, c.211_212insA; p.I71Nfs*246, caused by a one-nucleotide duplication that gave rise to a premature stop codon at amino acid 316. Her father and elder sister also harboured the identical *PAX9* variant, as confirmed by Sanger sequencing (Figure 2a).

The proband of family #356 carried a two-nucleotide heterozygous insertion variant, c.236_237insAC; p.T80Lfs*6, which resulted in the occurrence of a premature stop codon at amino acid 85. Sanger sequencing revealed that she inherited this frameshift variant from her mother who also suffered from NSO (Figure 2b).

Another *PAX9* missense variant, c.229C > G; p.R77G, was identified in the proband of family #348. The nucleotide sequence showed a heterozygous C to G transition at nucleotide 229, leading to the substitution of arginine to glycine at the position of residue 77 (Figure 2c). The potential pathogenicity of this missense variant was predicted to be deleterious (with a score of −6.981) or probably damaging (with a score of 0.994) by PROVEAN and Polyphen-2, respectively (Table 1). We also performed conservation analysis and revealed that the affected arginine 77 was evolutionarily conserved among species (Figure 3b).

3.3 | Novel PAX9 variants caused distinct structural changes in the PD

We conducted homology modelling and 3-dimensional structural analysis to assess the conformational changes and functional impacts of PAX9 variants. We predicted the conformation of the wild-type PD domain, composed of two distinct helix-turn-helix subdomains connected by a linker, as shown in Figure 4a. Of note, the three novel variants mainly caused varying degrees of conformational differences in the C-subdomain (Figure 4b-d, marked with red dotted boxes). When compared with the wild type, the p.I71Nfs*246 variant led to the disappearance of the third helix in the C-subdomain, as well as the conversion of the first helix into a loop (Figure 4b). More seriously, the p.T80Lfs*6 variant caused the entire loss of the C-subdomain (Figure 4c). Additionally, the p.R77G variant caused arginine, a positively charged amino acid with a longer molecular chain, to be substituted by an uncharged glycine at residue 77 (Figure 4d). Thus, results from the 3-dimensional structural analysis suggested that the diverse alterations of PAX9 variants might damage the interaction with other critical tooth developmental regulating signal molecules, such as BMP4, possibly by affecting their biological functions during tooth development.

3.4 | Novel frameshift variants of PAX9 affected the nuclear localization of PAX9

Successful expression of wild type and three variant PAX9 fusion proteins were detected by Western blotting (Figure 4t). Then, to investigate the functional impacts of PAX9 variants, we examined whether the nuclear localization of the expressed protein was affected. Fluorescence microscopy revealed that R77G variant specifically distributed in the nuclear of transient transfected 293T cells, similar to the localization of wild-type PAX9, whereas the variants of I71Nfs*246 and T80Lfs*6 were expressed in both cell nuclear and cytoplasm (Figure 4e–s).
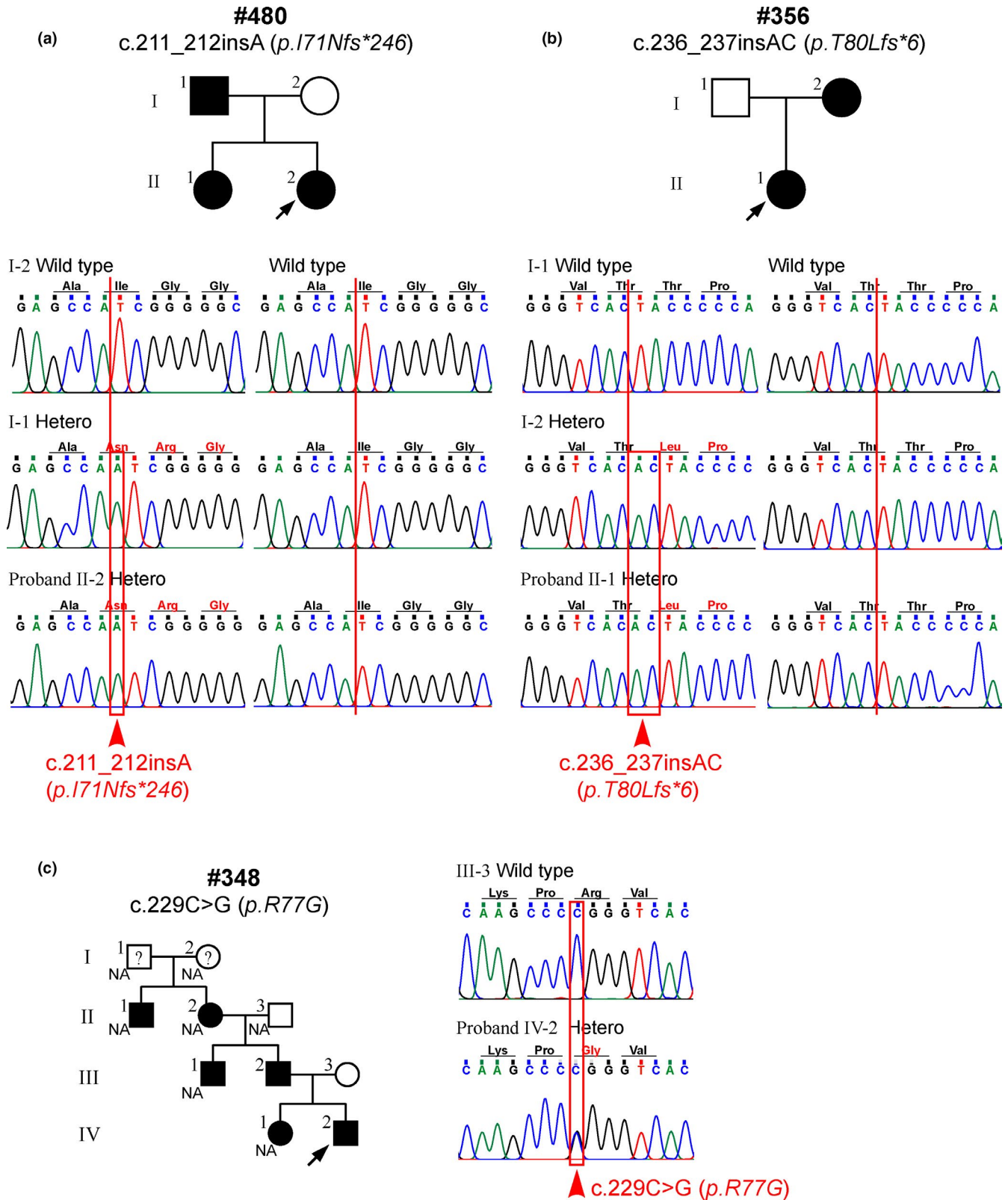
FIGURE 2 Pedigrees and genetic analyses of NSO families with *PAX9* variants. (a) Sequencing chromatograms of available DNA in family #480 present a heterozygous *PAX9* frameshift variant (c.211_212insA; p.I71Nfs*246) identified in the proband (II-2) and her father (I-1). (b) Sequencing chromatograms of available DNA in family #356 also present a heterozygous *PAX9* frameshift variant (c.236_237insAC; p.T80Lfs*6) identified in the proband (II-1) and her mother (I-2). (c) Sequencing chromatograms of available DNA in family #348 present a heterozygous *PAX9* missense variant (c.229C > G; p.R77G) identified in the proband (IV-2). Solid circles and squares represent the individuals with NSO. Black arrows indicate the probands. NA indicates that DNA samples are unavailable. Question marks (?) indicate that the oral phenotype is untraceable. All mutated nucleotides are framed in red [Colour figure can be viewed at wileyonlinelibrary.com]

FIGURE 3 Location and bioinformatic analyses of novel PAX9 variants. (a) Schematic diagram and distribution of variants in the PAX9 protein. Novel variants are indicated by arrows. (b) Conservation analysis of the 77th affected amino acid in the PAX9 protein among 10 different vertebrate species [Colour figure can be viewed at wileyonlinelibrary.com]
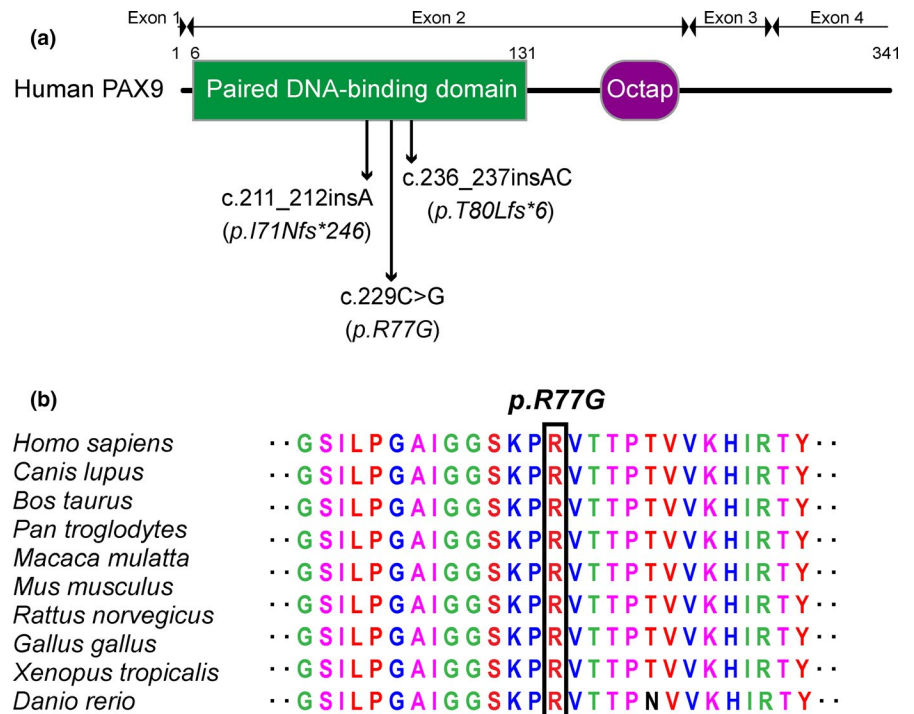
3.5 | Novel PAX9 variants severely reduced the activation of BMP4

BMP4 was recently identified to be one of the downstream targets of *PAX9* during the process of tooth development (Mitsui et al., 2014; Wong et al., 2018). Therefore, we investigated the transcriptional activation of *BMP4* to further explore the pathogenic mechanism of *PAX9*-related NSO. The luciferase results indicated that the transactivation capacity of *PAX9* to the *BMP4* promoter was significantly decreased in p.I71Nfs*246, p.T80Lfs*6 and p.R77G, when compared with the wild-type group ($p < .05$) (Figure 4u).

4 | DISCUSSION

Tooth development is controlled by the coordinated functions of numerous genes that are involved in dental epithelial–mesenchymal interactions. Alterations in any single gene may underlie tooth malformation or even TA (Murakami et al., 2017). However, the precise molecular pathways and gene–gene synergisms responsible for the occurrence of TA still require deep exploration. Given that *PAX9* variants are identified in 9% of the NSTA cases, only second to WNT10A (the detection rate was 56% in NSTA cases) (van den Boogaard et al., 2012), the continuous discovery of novel *PAX9* variants can help us gain a better understanding of the genetic mechanisms of tooth development. Our study described the identification of three hitherto unknown *PAX9* variants in individuals with autosomal-dominant NSO, including two frameshift variants (c.211_212insA; p.I71Nfs*246 and c.236_237insAC; p.T80Lfs*6) and one missense variant (c.229C > G; p.R77G). All identified variants resided within the PD, the DNA-binding domain of PAX9, and were

predicted to affect evolutionarily conserved amino acid residues. This distribution corresponds with the germline variant hot spot of *PAX9* that correlated with NSO (Liang et al., 2016), considering that approximately half (26/53) of the *PAX9* variants found in previous studies reside in the PD (Bonczek et al., 2017; Daw et al., 2017; Koskinen et al., 2019; Sarkar et al., 2017; Wong et al., 2018; Zhang et al., 2019). Since our results support the viewpoint that the evolutionarily conserved region closely interrelates with most of the variant hot spots, the *PAX9* hot spot region can be prioritized for variant screening (Walker et al., 1999). Our results further imply that the PD is the main functional domain in PAX9 that regulates the tooth development.

Despite extensive progress on the aetiology of oligodontia in molecular genetics, a significant issue remains to be resolved regarding the phenotypic variability of NSO, and more specifically, how certain gene variants, or different variants in the same gene, cause diverse missing teeth positions. Studies examining the genotype–phenotype correlation revealed that variants in different genes demonstrated quite distinct agenesis patterns in tooth position. To summarize, *EDA* variants typically result in the agenesis of lateral incisors and mandibular central incisors; however, *MSX1* or *WNT10A* variants generally affect the maxillary and mandibular second premolars (Fournier et al., 2018). For *PAX9* variants, the typical tooth phenotypes are summarized as follows: (a) 91.67% of patients with *PAX9* variants are diagnosed with autosomal-dominant NSO (Fournier et al., 2018; Gabris et al., 2006; Rolling & Poulsen, 2001); (b) the anterior teeth are the least affected whereas the maxillary and mandibular posterior regions are most affected, and the most striking feature associated with *PAX9* variants is the frequent agenesis of second molars (more than 80%) (Fournier et al., 2018; Kim et al., 2006); (c) bilaterally symmetrical agenesis is a particular form

TABLE 1 Summary of three novel *PAX9* variants in NSO patients and predicted results of functional changes

Proband Sex/Age (yrs)	Exon/Domain	Nucleotide/Protein change	Variant/Hereditary	Tooth position involvement	Number of missing teeth	PROVEAN	PolyPhen-2	ExAC	ACMG Classification (evidence of pathogenicity)
#480 F/14	2 PD	c.211_212insA/p.I71Nfs*246	Frameshift/parental	Molars, premolars, anterior teeth	18	–	–	Not present	Pathogenic PVS1 + PS3+PM1 + PM2+PP1
#356 F/22	2 PD	c.236_237insAC/p.T80Lfs*6	Frameshift/parental	Molars dominating	16	–	–	Not present	Pathogenic PVS1 + PS3+PM1 + PM2+PP1
#348 M/22	2 PD	c.229C > G/p.R77G	Missense/parental	Molars dominating	13	-6.981 Deleterious	0.994 Probably damaging	Not present	Likely pathogenic PS3 + PM1+PM2 + PP3

Note: –, not available.

in individuals harbouring *PAX9* variants; (d) some of the affected individuals also have morphological anomalies in their remaining teeth, which mainly manifests as microdontia and cone-shaped teeth (Lammi et al., 2003; Nieminen et al., 2001; Wang et al., 2011). Consistent with previous conclusions, the missing teeth positions of our probands predominantly distributed in the molar region, symmetrically. This suggests that *PAX9* plays a unique role in the development of molars. Besides, in contrast to the other two cases, the proband of family #480 presented a more severe agenesis in the anterior region, which indicates that different variant types within the same gene may lead to subtle changes in transcription products or downstream signals, and consequently cause different phenotypes in NSO. It is noteworthy that the strategy of looking only at genes related to tooth development is an advantage but also a limitation because it does not allow the discovery of new genes with potential role in odontogenesis. However, identification of new clinical pathogenic genes requires large and proper family pedigrees, and it is quite difficult to investigate unknown variants from unrelated sporadic patients with no consanguinity.

Through protein conformational analysis, we found the p.I71Nfs*246, p.T80Lfs*6 and p.R77G resulted in extreme structural disorders in the PD of PAX9 protein, manifesting as different degrees of C-subdomain deletion in the I71Nfs*246 and T80Lfs*6 variants, and a disruption in the coordination between the N-subdomain and C-subdomain in the R77G variant. These conformational changes suggest that the impaired DNA-binding ability of PAX9, influenced by the protein structure, plays a vital role in the failure of tooth formation in NSO patients.

To further elucidate the pathogenic mechanisms of *PAX9* variants, we performed functional analyses with respect to subcellular localization and *BMP4* promoter binding ability. Our results showed that all the PAX9 variants were detected at predicted size, suggesting that these variants were stable in vitro. However, only R77G variants presented uniform distribution within nuclear of 293T cells, whereas the GFP signals of I71Nfs*246 and T80Lfs*6 variants were observed in both nuclear and cytoplasms, indicating that the nuclear localization of frameshift variants was impaired. Therefore, PAX9 frameshift variants may lead to much lower efficiency on binding and regulating the downstream target genes.

BMP4 is a promising candidate gene for TA in humans and acts as a downstream signal molecule of *PAX9* (Jia et al., 2013; Yu et al., 2019). The importance of *BMP4* in tooth morphogenesis has been demonstrated in vivo. Homozygous *Pax9*-deficient mice showed tooth developmental arrest, accompanied by markedly reduced *Bmp4* expression in the dental mesenchyme, whereas the transgenic expression of *Bmp4* partially rescued the tooth dysplasia on *Pax9*-deficient mice (Nakatomi et al., 2010; Peters et al., 1998). An in vitro study demonstrated that *PAX9* activated the *BMP4* gene promoter by synergistically forming a heterodimeric complex with *MSX1* (Ogawa et al., 2006). Consistent with the previous findings (Mitsui et al., 2014), our luciferase results demonstrated that three identified PAX9 variants affected DNA-binding and *BMP4* promoter transactivation, suggesting that the
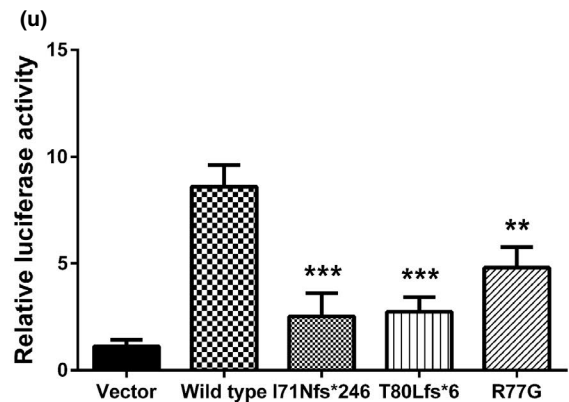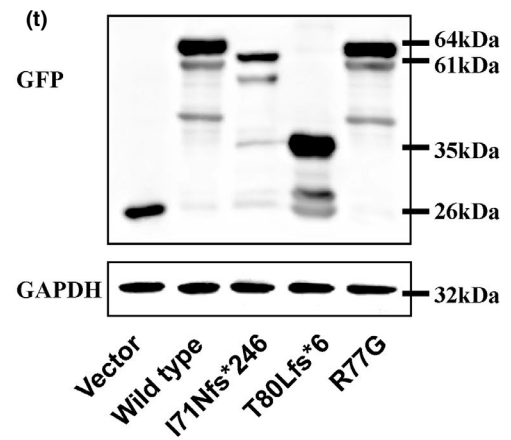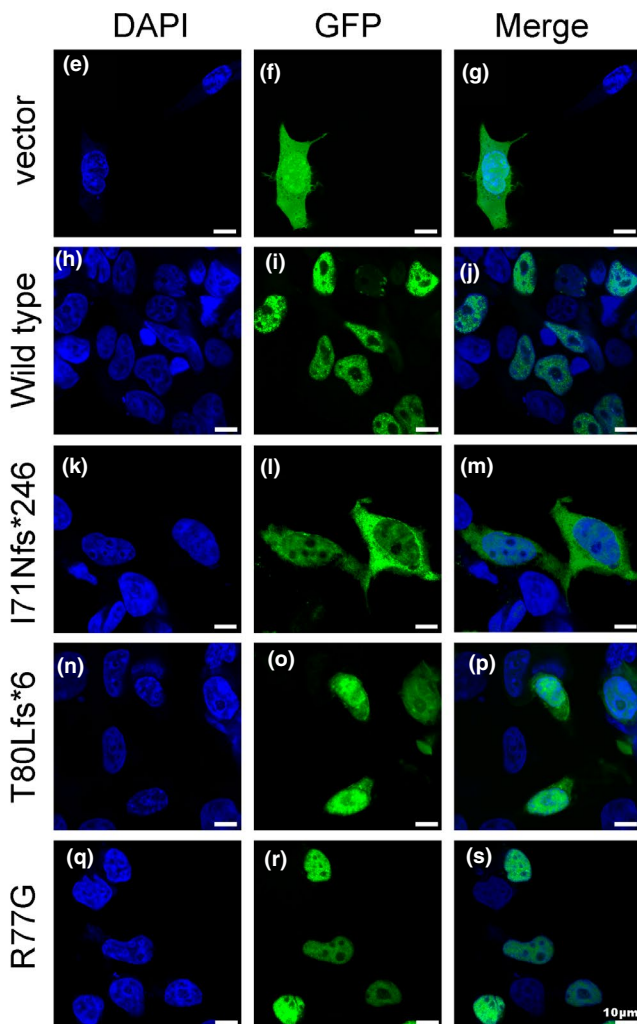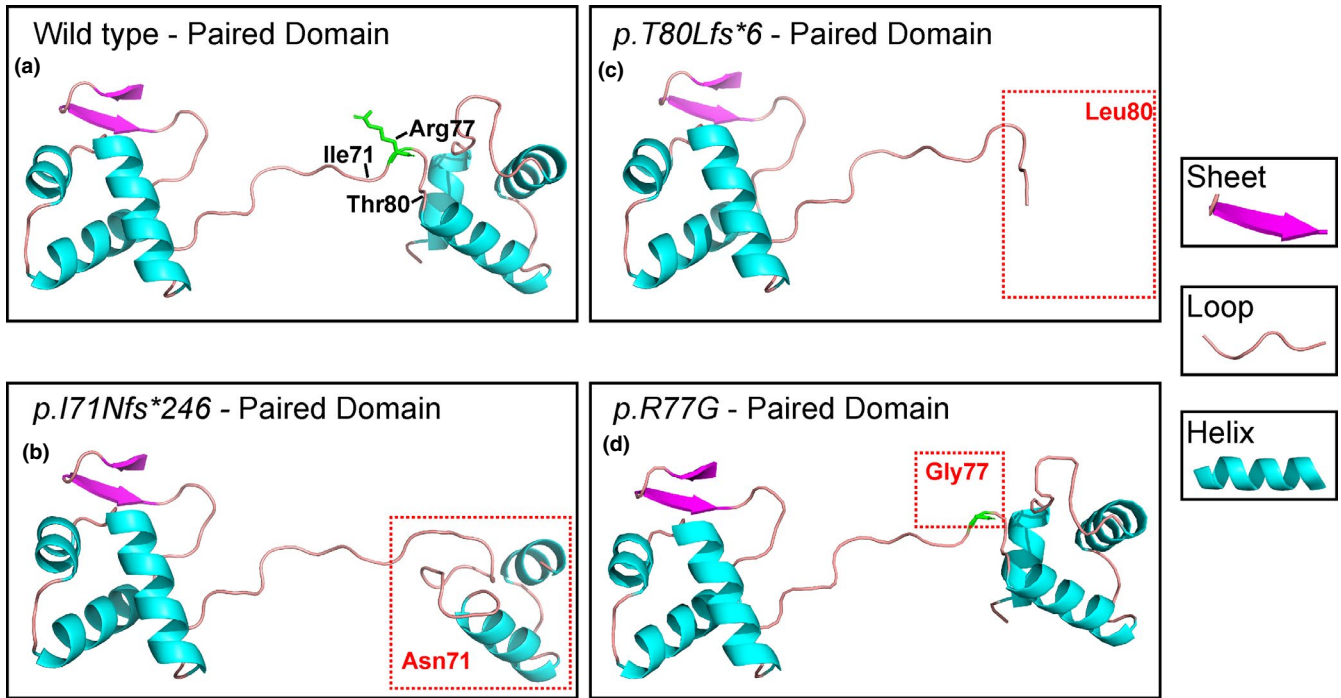
FIGURE 4 Protein conformational analysis and in vitro functional studies of PAX9 variants. (a) Tertiary structural modelling of the paired domain in wild-type PAX9 protein. (b–d) Predicted tertiary structural changes in the three altered proteins, I71Nfs*246 (b), T80Lfs*6 (c) and R77G (d), are boxed with red dotted lines. (e–s) Fluorescence microscopy demonstrates the subcellular localization of wild-type (h––j) and PAX9 variants: I71Nfs*246 (k-m), T80Lfs*6 (n–p) and R77G (q–s). GFP (green) for PAX9 expression, and DAPI (blue) for nuclear staining. (t) Expressions of wild-type and altered PAX9 proteins detected by Western blotting. An empty vector was used as a negative control. (u) Transactivation activity of PAX9 variants on the *BMP4* promoter, as assessed by luciferase reporter assay. Asterisks denote a statistically significant difference ($p < .05$), compared to the wild-type group. All data are expressed as means $\pm$ *SD* [Colour figure can be viewed at wileyonlinelibrary.com]

dominant-negative effect might be the underlying pathogenic mechanism in *PAX9*-related NSO. However, further studies are required to give insight into how the variants impact tooth development in *PAX9*-related NSO patients.

In conclusion, our study identified three hitherto unknown variants in the PD of PAX9, which extended the *PAX9* variant spectrum in NSO. Subsequent bioinformatic and functional studies confirmed that PD structural changes and the dominant-negative effect contributed to NSO in patients with *PAX9* variants. Continuous decoding of genetic aetiologies to reveal molecular mechanisms and further in-depth analyses of genotype–phenotype relationships will facilitate the early diagnosis, clinical intervention and treatment of TA, thus improving the oral health and quality of life of patients.

CONFLICT OF INTEREST

The authors declared no conflicts of interest.

AUTHOR CONTRIBUTION

Kai Sun: Data curation; Formal analysis; Investigation; Methodology; Writing-original draft. Miao Yu: Formal analysis. Iting Yeh: Formal analysis. Liutao Zhang: Investigation. Haochen Liu: Investigation. Tao Cai: Formal analysis; Investigation. Hailan Feng: Conceptualization; Funding acquisition; Project administration; Resources; Supervision; Validation; Writing-review & editing. Dong Han: Conceptualization; Funding acquisition; Project administration; Resources; Supervision; Validation; Writing-review & editing.

PEER REVIEW

The peer review history for this article is available at https://publons.com/publon/10.1111/odi.13684.

ORCID

Kai Sun https://orcid.org/0000-0002-0552-970X
Miao Yu https://orcid.org/0000-0001-8608-8354
Liutao Zhang https://orcid.org/0000-0002-1637-3771
Hailan Feng https://orcid.org/0000-0002-7640-5990
Yang Liu https://orcid.org/0000-0002-3940-3339
Dong Han https://orcid.org/0000-0001-9625-3384

REFERENCES

Bergendal, B., Klar, J., Stecksen-Blicks, C., Norderyd, J., & Dahl, N. (2011). Isolated oligodontia associated with mutations in EDARADD, AXIN2, MSX1, and PAX9 genes. *American Journal of Medical Genetics A*, *155A*(7), 1616–1622. https://doi.org/10.1002/ajmg.a.34045

Bonczek, O., Balcar, V. J., & Šerý, O. (2017). PAX9 gene mutations and tooth agenesis: A review. *Clinical Genetics*, *92*(5), 467–476. https://doi.org/10.1111/cge.12986

Daw, E. M., Saliba, C., Grech, G., & Camilleri, S. (2017). A novel PAX9 mutation causing oligodontia. *Archives of Oral Biology*, *84*, 100–105. https://doi.org/10.1016/j.archoralbio.2017.09.018

Fournier, B. P., Bruneau, M. H., Toupenay, S., Kerner, S., Berdal, A., Cormier-Daire, V., Hadj-Rabia, S., Coudert, A. E., & de La Dure-Molla, M. (2018). Patterns of dental agenesis highlight the nature of the causative mutated genes. *Journal of Dental Research*, *97*(12), 1306–1316. https://doi.org/10.1177/0022034518777460

Gabris, K., Fabian, G., Kaan, M., Rozsa, N., & Tarjan, I. (2006). Prevalence of hypodontia and hyperdontia in paedodontic and orthodontic patients in Budapest. *Community Dental Health*, *23*(2), 80–82.

Jia, S., Zhou, J., Gao, Y., Baek, J. A., Martin, J. F., Lan, Y., & Jiang, R. (2013). Roles of Bmp4 during tooth morphogenesis and sequential tooth formation. *Development*, *140*(2), 423–432. https://doi.org/10.1242/dev.081927

Jumlongras, D., Lin, J. Y., Chapra, A., Seidman, C. E., Seidman, J. G., Maas, R. L., & Olsen, B. R. (2004). A novel missense mutation in the paired domain of PAX9 causes non-syndromic oligodontia. *Human Genetics*, *114*(3), 242–249. https://doi.org/10.1007/s00439-003-1066-6

Kim, J. W., Simmer, J. P., Lin, B. P., & Hu, J. C. (2006). Novel MSX1 frameshift causes autosomal-dominant oligodontia. *Journal of Dental Research*, *85*(3), 267–271. https://doi.org/10.1177/154405910608500312

Koskinen, S., Keski-Filppula, R., Alapulli, H., Nieminen, P., & Anttonen, V. (2019). Familial oligodontia and regional odontodysplasia associated with a PAX9 initiation codon mutation. *Clinical Oral Investigations*, *23*(11), 4107–4111. https://doi.org/10.1007/s00784-019-02849-5

Lammi, L., Halonen, K., Pirinen, S., Thesleff, I., Arte, S., & Nieminen, P. (2003). A missense mutation in PAX9 in a family with distinct phenotype of oligodontia. *European Journal of Human Genetics*, *11*(11), 866–871. https://doi.org/10.1038/sj.ejhg.5201060

Liang, J., Qin, C., Yue, H., He, H., & Bian, Z. (2016). A novel initiation codon mutation of PAX9 in a family with oligodontia. *Archives of Oral Biology*, *61*, 144–148. https://doi.org/10.1016/j.archoralbio.2015.10.022

Liu, H., Han, D., Wong, S., Nan, X., Zhao, H., & Feng, H. (2013). rs929387 of GLI3 is involved in tooth agenesis in Chinese Han population. *PLoS One*, *8*(11), e80860. https://doi.org/10.1371/journal.pone.0080860

Mitsui, S. N., Yasue, A., Masuda, K., Watanabe, K., Horiuchi, S., Imoto, I., & Tanaka, E. (2014). Novel PAX9 mutations cause non-syndromic tooth agenesis. *Journal of Dental Research*, *93*(3), 245–249. https://doi.org/10.1177/0022034513519801

Murakami, A., Yasuhira, S., Mayama, H., Miura, H., Maesawa, C., & Satoh, K. (2017). Characterization of PAX9 variant P20L identified in a Japanese family with tooth agenesis. *PLoS One*, *12*(10), e0186260. https://doi.org/10.1371/journal.pone.0186260

Nakatomi, M., Wang, X.-P., Key, D., Lund, J. J., Turbe-Doan, A., Kist, R., Aw, A., Chen, Y., Maas, R. L., & Peters, H. (2010). Genetic interactions

between Pax9 and Msx1 regulate lip development and several stages of tooth morphogenesis. *Developmental Biology*, *340*(2), 438–449. https://doi.org/10.1016/j.ydbio.2010.01.031

Nieminen, P., Arte, S., Tanner, D., Paulin, L., Alaluusua, S., Thesleff, I., & Pirinen, S. (2001). Identification of a nonsense mutation in the PAX9 gene in molar oligodontia. *European Journal of Human Genetics*, *9*(10), 743–746. https://doi.org/10.1038/sj.ejhg.5200715

Ogawa, T., Kapadia, H., Feng, J. Q., Raghow, R., Peters, H., & D'Souza, R. N. (2006). Functional consequences of interactions between Pax9 and Msx1 genes in normal and abnormal tooth development. *Journal of Biological Chemistry*, *281*(27), 18363–18369. https://doi.org/10.1074/jbc.M601543200

Peters, H., Neubuser, A., Kratochwil, K., & Balling, R. (1998). Pax9-deficient mice lack pharyngeal pouch derivatives and teeth and exhibit craniofacial and limb abnormalities. *Genes and Development*, *12*(17), 2735–2747. https://doi.org/10.1101/gad.12.17.2735

Polder, B. J., Van't Hof, M. A., Van der Linden, F. P., & Kuijpers-Jagtman, A. M. (2004). A meta-analysis of the prevalence of dental agenesis of permanent teeth. *Community Dentistry and Oral Epidemiology*, *32*(3), 217–226. https://doi.org/10.1111/j.1600-0528.2004.00158.x

Prasad, M. K., Geoffroy, V., Vicaire, S., Jost, B., Dumas, M., Le Gras, S., Switala, M., Gasse, B., Laugel-Haushalter, V., Paschaki, M., Leheup, B., Droz, D., Dalstein, A., Loing, A., Grollemund, B., Muller-Bolla, M., Lopez-Cazaux, S., Minoux, M., Jung, S., … Bloch-Zupan, A. (2016). A targeted next-generation sequencing assay for the molecular diagnosis of genetic disorders with orodental involvement. *Journal of Medical Genetics*, *53*(2), 98–110. https://doi.org/10.1136/jmedgenet-2015-103302

Richards, S., Aziz, N., Bale, S., Bick, D., Das, S., Gastier-Foster, J., Grody, W. W., Hegde, M., Lyon, E., Spector, E., Voelkerding, K., & Rehm, H. L. (2015). Standards and guidelines for the interpretation of sequence variants: A joint consensus recommendation of the American College of Medical Genetics and Genomics and the Association for Molecular Pathology. *Genetics in Medicine: Official Journal of the American College of Medical Genetics*, *17*(5), 405–424. https://doi.org/10.1038/gim.2015.30

Rolling, S., & Poulsen, S. (2001). Oligodontia in Danish schoolchildren. *Acta Odontologica Scandinavica*, *59*(2), 111–112. https://doi.org/10.1080/000163501750157298

Sarkar, T., Bansal, R., & Das, P. (2017). A novel G to A transition at initiation codon and exon-intron boundary of PAX9 identified in association with familial isolated oligodontia. *Gene*, *635*, 69–76. https://doi.org/10.1016/j.gene.2017.08.020

Stockton, D. W., Das, P., Goldenberg, M., D'Souza, R. N., & Patel, P. I. (2000). Mutation of PAX9 is associated with oligodontia. *Nature Genetics*, *24*(1), 18–19. https://doi.org/10.1038/71634

Thimmegowda, U., Prasanna, P., Athimuthu, A., Bhat, P. K., & Puttashamachari, Y. (2015). A nonsyndromic autosomal dominant oligodontia with a novel mutation of PAX9-A clinical and genetic report. *Journal of Clinical and Diagnostic Research*, *9*(6), Zd08-Zd10. https://doi.org/10.7860/jcdr/2015/13173.6049

van den Boogaard, M. J., Créton, M., Bronkhorst, Y., van der Hout, A., Hennekam, E., Lindhout, D., & Ploos van Amstel, H. K. (2012). Mutations in WNT10A are present in more than half of isolated hypodontia cases. *Journal of Medical Genetics*, *49*(5), 327–331. https://doi.org/10.1136/jmedgenet-2012-100750

Vieira, A. R., Meira, R., Modesto, A., & Murray, J. C. (2004). MSX1, PAX9, and TGFA contribute to tooth agenesis in humans. *Journal of Dental Research*, *83*(9), 723–727. https://doi.org/10.1177/154405910408300913

Vogan, K. J., & Gros, P. (1997). The C-terminal subdomain makes an important contribution to the DNA binding activity of the Pax-3 paired domain. *Journal of Biological Chemistry*, *272*(45), 28289–28295. https://doi.org/10.1074/jbc.272.45.28289

Walker, D. R., Bond, J. P., Tarone, R. E., Harris, C. C., Makalowski, W., Boguski, M. S., & Greenblatt, M. S. (1999). Evolutionary conservation and somatic mutation hotspot maps of p53: Correlation with p53 protein structural and functional features. *Oncogene*, *18*(1), 211–218. https://doi.org/10.1038/sj.onc.1202298

Wang, J., Jian, F., Chen, J., Wang, H. U., Lin, Y., Yang, Z., Pan, X., & Lai, W. (2011). Sequence analysis of PAX9, MSX1 and AXIN2 genes in a Chinese oligodontia family. *Archives of Oral Biology*, *56*(10), 1027–1034. https://doi.org/10.1016/j.archoralbio.2011.03.023

Wang, J., Sun, K. E., Shen, Y., Xu, Y., Xie, J., Huang, R., Zhang, Y., Xu, C., Zhang, X. U., Wang, R., & Lin, Y. (2016). DNA methylation is critical for tooth agenesis: Implications for sporadic non-syndromic anodontia and hypodontia. *Scientific Reports*, *6*, 19162. https://doi.org/10.1038/srep19162

Wong, S. W., Han, D., Zhang, H., Liu, Y., Zhang, X., Miao, M. Z., & Feng, H. (2018). Nine novel pax9 mutations and a distinct tooth agenesis genotype-phenotype. *Journal of Dental Research*, *97*(2), 155–162. https://doi.org/10.1177/0022034517729322

Wong, S., Liu, H., Bai, B., Chang, H., Zhao, H., Wang, Y., Han, D., & Feng, H. (2014). Novel missense mutations in the AXIN2 gene associated with non-syndromic oligodontia. *Archives of Oral Biology*, *59*(3), 349–353. https://doi.org/10.1016/j.archoralbio.2013.12.009

Yu, M., Wang, H., Fan, Z., Xie, C., Liu, H., Liu, Y., Han, D., Wong, S.-W., & Feng, H. (2019). BMP4 mutations in tooth agenesis and low bone mass. *Archives of Oral Biology*, *103*, 40–46. https://doi.org/10.1016/j.archoralbio.2019.05.012

Yu, P., Yang, W., Han, D., Wang, X. I., Guo, S., Li, J., Li, F., Zhang, X., Wong, S.-W., Bai, B., Liu, Y., Du, J., Sun, Z. S., Shi, S., Feng, H., & Cai, T. (2016). Mutations in WNT10B are identified in individuals with oligodontia. *American Journal of Human Genetics*, *99*(1), 195–201. https://doi.org/10.1016/j.ajhg.2016.05.012

Zeng, B., Zhao, Q. I., Li, S., Lu, H., Lu, J., Ma, L., Zhao, W., & Yu, D. (2017). Novel EDA or EDAR mutations identified in patients with X-linked hypohidrotic ectodermal dysplasia or non-syndromic tooth agenesis. *Genes (Basel)*, *8*(10), 259. https://doi.org/10.3390/genes8100259

Zhang, J., Liu, H. C., Lyu, X., Shen, G. H., Deng, X. X., Li, W. R., & Feng, H. L. (2015). Prevalence of tooth agenesis in adolescent Chinese populations with or without orthodontics. *Chinese Journal of Dental Research*, *18*(1), 59–65.

Zhang, T., Zhao, X., Hou, F., Sun, Y., Wu, J., Ma, T., & Zhang, X. (2019). A novel PAX9 mutation found in a Chinese patient with hypodontia via whole exome sequencing. *Oral Diseases*, *25*(1), 234–241. https://doi.org/10.1111/odi.12982

SUPPORTING INFORMATION

Additional supporting information may be found online in the Supporting Information section.